Author/s:
Guo, Y;Karimi, F;Fu, Q;G Qiao, G;Zhang, H

Title:
Reduced administration frequency for the treatment of fungal keratitis: a sustained natamycin release from a micellar solution.

Date:
2020-02-03

Citation:
Guo, Y., Karimi, F., Fu, Q., G Qiao, G. & Zhang, H. (2020). Reduced administration frequency for the treatment of fungal keratitis: a sustained natamycin release from a micellar solution.. Expert Opin Drug Deliv, 17 (3), pp.407-421. https://doi.org/10.1080/17425247.2020.1719995.

Reduced administration frequency for the treatment of fungal keratitis: A sustained natamycin release from a micellar solution

Yiyuan Guo,[1,2a] Fatemeh Karimi,[2,3a] Qiang Fu,[2,4] Greg. G. Qiao,[2*] Hong Zhang,[1*]

[1]Department of Ophthalmology, The First Affiliated Hospital of Harbin Medical University, Harbin, Peoples Republic of China

[2]Department of Chemical Engineering, The University of Melbourne, Victoria 3010, Australia

[3]Graduate School of Biomedical Engineering, University of New South Wales, Sydney, NSW 2052, Australia

[4]The Centre for Technology in Water and Wastewater (CTWW), School of Civil and Environmental Engineering, University of Technology Sydney, NSW 2007 Australia

[a] Authors contributed equally

[*] Corresponding Authors:

Hong Zhang

Department of Ophthalmology, The First Affiliated Hospital of Harbin Medical University, NO.25, Youzheng Street, Harbin,150086

Phone: +86-13804505456; e-mail: 13804505456@163.com

Greg Qiao

Department of Chemical Engineering, The University of Melbourne, Parkville 3010, Victoria, 3010

26 Phone: +61 3 8344 8665; e-mail: gregghq@unimelb.edu.au

Abstract

We report the synthesis and preparation of self-assembled poly(ethylene glycol)-block-poly(glycidyl methacrylate) (PEG-*b*-PGMA) micelles harnessing the intrinsically hydrolysable characteristics of PGMA segments for the sustained delivery of a hydrophobic natamycin by topical administration on eye. Hydrolysis of the glycidyl groups could be achieved within physiologically relevant environment, resulting in increased drug release compared to conventional non-hydrolysable counterparts. It was found that the system provides an additional driving force for drug release by generation of hydrophilic hydroxyl groups to "push" the encapsulated hydrophobic drug away from the hydrophobic domains and into the surrounding environments. *In vitro and in vivo* results revealed that the drug carriers (PEG-*b*-PGMA micelles) and the encapsulated natamycin were not cytotoxic to human corneal epithelial cells and the released drug have strong antifungal ability to *Candida albicans*. Importantly, sustained natamycin release from micelles leads to the reduced administration frequency of natamycin from 8 times per day to 3 times per day in fungal keratitis (FK) rabbits. Corneal morphology of keratitis was improved by the release of natamycin from the micelle observed by anterior segment optical coherence tomography (AS-OCT) and histological analysis of the cornea. These results revealed that the use of micelle enhances the loading and delivery efficiency of natamycin and subsequently promotes the drug penetration in aqueous humor and cornea. The present study demonstrates a facile method that can greatly reduce dosing frequency of natamycin administration and thus improve long-term patient compliance.

Keywords: Micelle; Natamycin; Eye drop; Sustained release; Fungal keratitis

1. Introduction

Fungal keratitis (FK) is a severe corneal fungal infection that occurs worldwide. This can lead to permanent vision loss and even total blindness or corneal perforation (endophthalmitis) when not diagnosed early and immediately treated [1]. The predisposing factors that involve ocular trauma are associated with agricultural matter in rural areas and contact lens use in developed countries. Other risk factors include the disproportionate use of broad spectrum antibiotics, steroid drops, and increased number of eye surgeries that frequently touch the corneal surface [1],[2]. *Aspergillus*, *Candida*, and *Fusarium* species are the three major groups of fungus that cause FK [2]. These usually produce serious pathological changes including immune rings, satellite lesions, pseudopods, hypha moss, hypopyon and endothelial plaques [3].

Natamycin which is the only commercially available agent approved by Food and Drug Administration (FDA) for treating FK [4] has been considered as one of the most valuable agents for experimental research. Compared with other antifungal drugs such as fluconazole and amphotericin B, natamycin has the advantages of good antifungal effect and less adverse reactions [5],[6]. Natamycin is a hydrophobic drug with low water solubility and 5% w/v natamycin suspension is clinically prescribed as one drop instilled in the conjunctival sac at hourly or two hourly intervals for 3-4 days and at 6-8 times daily for 14-21 days [7]. Due to aforementioned reasons and tear wash, a high dosing frequency is required which leads patient noncompliance and cited as the leading problem in treating FK. Hence, there is an urgent clinical need to design a corneal targeted prolonged release delivery system to reduce the dosing frequency of natamycin.

A variety of drug carriers including cyclodextrin and cell penetrating peptide have been explored for the sustained release of natamycin [8], [9], [10], [11]. Anjali *et*

al. reported the cyclodextrins can improve the aqueous stability of natamycin and hence reduce local irritation [8]. Jain *et al.* reported that the conjugation between natamycin and cell penetrating peptide leads to the enhanced solubility of the drug in aqueous medium [10]. However, issues have emerged due to the instability, incomplete inclusion, non-specificity and rapid intracellular degradation [10],[12]. Recently, great effort has been made to design and fabricate polymeric nanoparticles owing to their ability to encapsulate and release drugs on demand under specific conditions [13], [14].Micelles have been considered as a good drug delivery carrier due to their sustained release capacity and special characteristics [15]. Micelle which usually be achieved by the self-assembly of block co-polymers is an amphipathic nano-sized carrier with a core-shell structure. The hydrophobic core offers the entrapment of the hydrophobic drug serving as a drug reservoir and the hydrophilic shell forms a steric barrier to the micelle aggregation, which ensures the solubility of micelles in an aqueous or biological environment. Therefore, the use of micelles for the hydrophobic drug encapsulation could directly increase the water-solubility of hydrophobic drugs in aqueous media and subsequently enhance the drug delivery efficiency [16],[17], [18], [19]. In addition, micelles can be tailored to achieve a sustained or on-demand drug release pattern by controlling the composition, functionality, size, and overall morphology [20].

In the present study, we report a straightforward method to initiate drug release where the environment itself is used to initiate intrinsic changes to the chemical structure of the micelles. These changes facilitate and enhance the drug release into the outer environment without entire particle degradation. In order to achieve this, we designed and synthesized a biocompatible poly(ethylene glycol)-block-poly(glycidyl methacrylate) (PEG-*b*-PGMA) micellar delivery system by incorporating glycidyl

methacrylate as a polymeric building block which has been widely explored for post-polymerization modifications through ring opening reactions of the epoxy group by a nucleophilic agent [21], [22]. Although incorporation of glycidyl methacrylate has been widely used as a platform for modification, to the best of our knowledge it has not been utilized as a facile method to intrinsically induce drug release in a sustained manner due to the hydrolysis of the epoxy rings to alter overall structural hydrophilicity. Therefore, we prepared the micelles via self-assembly of the block copolymers where partial of the epoxy groups were used for cross-linking to covalently stabilize the micelles and the remaining epoxy groups can undergo sustained hydrolysis in aqueous environments to enhance self-initiated drug release over prolonged time periods. Additionally, PEGylated shell of the micelles can enhance the contact time with the mucus layer of the tear film, act as mucoadhesion promoters and enhance the corneal penetration of the drug-loaded micelles [23], [24]. This system was used as a new delivery platform for the sustained and controlled long-term release of hydrophobic natamycin *in vitro* and *in vivo* to treat fungal keratitis.

2. Methods

2.1 Materials

Methoxy-PEG-amine, HCl salt (JenKem, M_n = 5 kDa), 4-Cyano-4-(((dodecylthio)carbonothioyl)thio)-pentanoic acid (Boron Molecular Pty Ltd). 4-dimethylaminopyridine (DMAP, 99%, Sigma-Aldrich), and 1-ethyl-3-(3-dimethylaminopropyl) carbodiimide (EDC, 99%, Sigma-Aldrich) were used as received. Glycidyl methacrylate (GMA, Sigma-Aldrich) was passed over the basic

alumina columns (Scharlau) to remove the inhibitors and stored at 2-8°C. 2,2'-Azobis(2-methylpropionitrile) (AIBN, 98%, ACROS ORGANICS) was used after recrystallization from methanol. Natamycin was purchased from Selleck Chemicals (Houston, USA). The *Candida albicans* (*C. albicans*, ATCC 10231) was a kind gift from Dr. Zhang (Department of Microbiology, Harbin Medical University, Harbin, China). The yeast extract peptone dextrose medium (YPD) broth was purchased from Meilunbio (Dalian, China). The human corneal epithelial (HCE-2) cell line was supplied by the American Type Culture Collection (ATCC, Manassas, USA). For the cell culture, the Dulbecco's Modified Eagle's Medium:nutrient mixture F12 (DMEM:F12) and phosphate-buffered saline (PBS) were purchased from Hyclone (Logan City, USA). The methyl thiazolyl tetrazolium (CCK-8) was purchased from Dojindo (Kumamoto Prefecture, Japan), while the pentobarbital sodium was obtained from Sigma-Chemical Co. (St. Louis, USA). The marketed tobramycin and dexamethasone eye ointment TobraDex®, levofloxacin eye drops Cravit® (Santen, Osaka, Japan) and oxybuprocaine hydrochloride eye drops Benoxil® (Santen, Osaka, Japan) were purchased from a local pharmacy store.

2.2 Polymer synthesis

Neutralization of methoxy-PEG-amine, HCl salt

Methoxy-PEG-amine, HCl salt (MeO-PEG-NH_2.HCl, 1 g, M_n = 5 k, JenKem) was dissolved in 20 mL of 0.1 M sodium hydroxide and stirred for two hours. Then, the neutralized MeO-PEG-NH_2 was extracted by dichloromethane (DCM, 50 mL ×2), washed with water (40 mL ×1), and dried over $MgSO_4$. Afterwards, the product was concentrated by removing the solvent under reduced pressure, precipitated in diethyl ether (DEE), and vacuum dried for over two days at R.T. (70-80 % Yield).

Synthesis of macro-raft agent (macro-TTC)

The methoxy-PEG-amine (0.7 g, 0.14 mmol), 4-cyano-4-(((dodecylthio)carbonothioyl)thio)-pentanoic acid (67.82 mg, 0.168 mmol), 4-dimethylaminopyridine (25.65 mg, 0.21 mmol), and 1-ethyl-3-(3-dimethylaminopropyl) carbodiimide (40.26 mg, 0.21 mmol) were dissolved in 25 mL anhydrous DCM, and allowed to react overnight at room temperature. Then, the reaction mixture was diluted with DCM (25 mL), washed with deionized water (50 mL ×1) and hydrochloric acid (0.5 M, 50 mL ×1), saturated with $NaHCO_3$ (50 mL ×1) and deionized water (50 mL ×1), further saturated with NaCl (50 mL ×1). The organic phase was isolated and dried over $MgSO_4$. Afterwards, the product (macro-TTC) was concentrated *via* rotary evaporation, precipitated in diethyl ether, and vacuum dried for over two days (yellow powder, 83% yield).

Synthesis of PEG-b-PGMA copolymer

The synthesis of PEG-*b*-PGMA copolymer was achieved via reversible addition-fragmentation chain transfer (RAFT) polymerization [25], [26]. Briefly, Macro-TTC (500 mg, 0.092 mmol), glycidyl methacrylate (GMA, 392.34 mg, 2.76 mmol), and an initiator (AIBN, 3.02 mg, 0.0184 mmol) were dissolved in 2.7 mL of DMSO (1:3 w/v ratio of macro-TTC and GMA to solvent). Then, the reaction mixture was transferred to a Schlenk flask with a stirrer bar and degassed by three freeze-pump-thaw cycles. Afterwards, the flask was back-filled with argon and stirred at 70°C for 19 hours. Subsequently, the polymerization was quenched by opening to air and cooling to room temperature. Then, the product was purified by precipitation in acetone:DEE (1:9 v/v) twice, dried under vacuum overnight, and stored at room temperature.

2.3 Hydrolysis of the glycidyl groups

The hydrolysis of glycidyl groups was conducted under mild physiological conditions. Briefly, 100 mg of PEG-*b*-PGMA copolymer was dissolved in 5 mL of PBS buffer (pH 7.4), and the solution was incubated in a glass vial at 37°C for over eight days. The purification of the resulted polymer was achieved by removing the water, re-dissolving in ACN (5 mL), and precipitating into cold DEE (50 mL ×2). Then, the product was collected by centrifugation and dried *in-vacuo* (0.1 mbar) for ^{1}H NMR spectroscopic analysis.

2.4 Micelle preparation

Self-assembly of PEG-b-PGMA into micelle

PEG-*b*-PGMA (100 mg, 0.01 mmol) was dissolved in 1 mL of tetrahydrofuran (THF), and 10 mL of non-solvent ethanol (EtOH) was added dropwise to the PEG-*b*-PGMA solution while continuously stirring. A turbid suspension was resulted, and the mixture was left stirring overnight at room temperature. Then, the THF was removed from the system by dialysis (ThermoFisher Scientific, MWCO: 3.5 kDa) against EtOH.

Covalent stabilization of self-assembled PEG-b-PGMA into cross-linked micelle

The obtained PEG-*b*-PGMA micelle solution (100 mg, 0.01 mmol) was concentrated to obtain a total volume of 3 mL. A solution of 1,7-diaminoheptane (9.27 mg, 0.079 mmol, 50 mol% of PGMA) was dissolved in 100 μL of THF and added dropwise to the continuously stirred solution of micelle suspension. The

reaction mixture was left mixing for three days, and subsequently dialyzed against EtOH to remove any unreacted cross-linker and THF.

2.5 Drug loading of cross-linked micelle

Next, 20 mg of natamycin was dissolved in 500 μL of DMSO and added dropwise to 3 mL of cross-linked micelle (100 mg, 0.01 mmol) in ethanol while continuously stirring. After two hours, the mixture was dialyzed against PBS (pH 7.4, 30 mL ×3) to remove any organic solvents and unloaded drug in micelle. UV-Vis spectroscopy was used to calculate the amount of unloaded drug in the solution using standard calibration curves generated from known drug concentrations (a 1:1 ratio of PBS-to-DMSO was used for both calibration curves and samples). Drug loading content (DLC) and drug loading efficiency (DLE) was calculated according to the following equations:

$$\mathrm{DLC} = \frac{\text{weight of loaded drug}}{\text{weight of carrier+weight of drug}} \times 100\% \qquad \text{Eq-1}$$

$$\mathrm{DLE} = \frac{\text{weight of loaded drug}}{\text{weight of total drug used}} \times 100\% \qquad \text{Eq-2}$$

2.6. *In vitro* release of drug from drug-loaded micelle

In vitro drug release was performed using the dialysis method. Briefly, the drug-loaded micelle (i.e. containing 10 mg of micelle + 1.88 mg of natamycin) were suspended in 5 mL of PBS at pH 7.4. Then, the solutions were transferred into a dialysis bag (MWCO 3.5 kDa) and dialyzed against PBS pH 7.4 (200 mL). Afterwards, the mixture was left stirring at 37°C to mimic the physiological conditions. At various intervals, 1-mL aliquots were taken from the outside of the

dialysis bag and diluted with 1 mL of DMSO for UV-Vis spectroscopy. The drug concentration was calculated according to the standard curve.

2.7. Characterization

***Nuclear Magnetic Resonance (NMR) Spectroscopy*:** Proton NMR (^{1}H NMR) analysis was conducted using a Varian Unity Plus 400 MHz spectrometer operating at 400 MHz. All samples were analyzed at a concentration of approx. 10 mg mL^{-1}, and deuterated chloroform was used as a reference.

***Gel Permeation Chromatography (GPC)*:** The GPC characterization of polymers was carried out using THF as the eluent. GPC analysis was performed using a modular Shimadzu system that comprised of a Shimadzu RID-10A interferometric refractometer (λ = 633 nm) using three Agilent MIXED-C columns (5-μm bead size) operating at 45°C.

***Transmission Electron Microscopy (TEM)*:** TEM images were taken using a Philips CM120 BioTWIN TEM at an operating voltage of 120 kV. The samples of the particles were air-dried on a carbon-coated Formvar film mounted on 300 mesh copper grids (ProSciTech, Australia).

***Dynamic light scattering (DLS)*:** Dynamic light scattering measurements were performed on a Zetasizer Nano ZS (Malvern Instruments). Analysis was performed at a constant temperature of 25°C.

***UV-Visible Spectroscopy*:** UV-Vis analysis was performed on a Shimadzu UV-1800 spectrometer using quartz cuvettes, with a 1-cm path length.

2.8 *In-vitro* studies

2.8.1 *In-vitro* cytotoxicity evaluation

Corneal epithelial cell culture

Human corneal epithelial (HCE-2) cells were maintained in DMEM/F-12 medium supplemented with 10% (v/v) fetal bovine serum (FBS), insulin (4 mg/mL), EGF (10 ng/mL), and penicillin–streptomycin (1%). Then, these cells were incubated in a humidified 5% CO_2 atmosphere at 37°C and sub-cultured at approximately 80% confluency using trypsin (0.05%). Afterwards, cells from passages 2-6 were used to perform the *in vitro* assays.

Cytotoxicity assay

HCE-2 cells were seeded into 96-well plates at an initial cell density of 8,000 cells/well and incubated at 37 °C. The drug-loaded micelle solution was diluted with cell culture medium at various concentrations of 12.50, 25.00, 50.00, 100.00, 200.00, 400.00 and 800.00 μg/mL, with natamycin concentrations of 2, 4, 8, 16, 32, 64 and 128 μg/ml, respectively. Pure natamycin with different concentrations (2, 4, 8, 16, 32, 64 and 128 μg/ml) was used as the control experiment. After 24 hours of cell culture, the medium was replaced with diluted drug-loaded micelle solution and pure natamycin solution, and further incubated for 24 and 72 hours. Then, these cells were washed twice with PBS, and further incubated with 110 μL of DMEM/F-12 containing 10 μL of CCK-8 solution for two hours. Finally, the medium was removed, and the absorbance at 450 nm was measured using a microplate reader (Bio-Rad, Japan). All experiments were performed in triplicate. The cell viability (%) was calculated using the following formula, where [*A*] is the average absorbance:

$$\text{Cell viability (\%)} = \frac{[A]_{450\ (\text{sample})} - [A]_{450\ (\text{blank})}}{[A]_{450\ (\text{control})} - [A]_{450\ (\text{blank})}}$$

2.8.2 *In-vitro* antifungal activity

Fungal cell culture (method of inoculation)

C. albicans was cultured on YPD plates and stored at 4°C for use. For amplification, a small inoculum from an isolated colony was selected with a sterile inoculating loop and suspended in a test tube containing YPD culture media by rubbing the inoculated loop against the wall of the test tube. This helps to dilute the pasty colonies by giving the media a turbid appearance. Then, the fungus was incubated in a humidified 5% CO_2 atmosphere at 37°C.

Minimum inhibitory concentration (MIC)

The MIC of natamycin-loaded micelle was determined following the guidelines of the Clinical and Laboratory Standards Institute [CLSI 2014] and a previously reported method [27], with slight modifications. Briefly, pure natamycin (64.00-0.25 µg/mL) and natamycin-loaded micelle (400.00-1.56 µg/mL, containing natamycin with concentrations within 64.00-0.25 µg/mL) were diluted with YPD using the double broth dilution method in the wells of 96-well microtiter plates. Then, a suspension ($[A]_{600}$ = 0.001) of *C. albicans* (10^4 CFU/mL) in YPD was added, with the appropriate negative (Ctrl 1 = media only, must clear) and positive (Ctrl 2 = *C. albicans* only in media, must contaminative) controls. Afterwards, these microtiter plates were incubated for 24 hours, and the white turbidity ($[A]_{600}$) were recorded using a microplate reader (Bio-Rad, Japan). The endpoint was defined as the lowest concentration of the compound that resulted in total inhibition of growth, when compared to the growth in negative control wells. All experiments were performed in triplicate. The fungus numbers (%) were calculated using the following formula, where [*A*] is the average absorbance:

$$\text{Fungus numbers (\%)} = \frac{[A]_{600\ (\text{sample})} - [A]_{600\ (\text{blank})}}{[A]_{600\ (\text{control})} - [A]_{600\ (\text{blank})}}$$

Zone of inhibition

Drug sensitivity to antifungal drugs was determined by disc diffusion assay. The *Candida* cells grew for 24 hours, and five colonies were selected. Then, these cells were counted and adjusted to a density of 10^6 CFU/mL. In order to obtain a confluent lawn of growth, 400 μL of this suspension was added and spread onto a YPD plate. Then, antibiotic disks containing natamycin (5 μg and 10 μg), natamycin-loaded micelle (containing 5 μg and 10 μg natamycin) and PBS were prepared and placed on the YPD plates. Afterwards, these plates were incubated for 24 hours at 37℃, and the inhibition zone was measured using a Vernier caliper.

2.9 *In-vivo* studies

2.9.1 Ocular irritation tests

Ocular irritation was evaluated according to the modified Draize test [28]. A total of six rabbits were divided into three groups, which included the control group and natamycin-loaded micelle group. Solutions that consisted of 80 mg/ml of natamycin-loaded micelle were instilled into the left eyes of rabbits, while blank PBS was instilled into the right eyes as controls. A single instillation of the sample (50 μl) every one hour at eight times per day lasted for a period of three days. The ocular tissues were observed at 0 and 72 hours after the last instillation by slit-lamp biomicroscopy. The corneal opacity was graded on a scale of 0-4 and iris hyperemia was graded on a scale of 0-2, while conjunctival congestion, swelling and discharge was graded on scales of 0–3, 0–4 and 0–3, respectively. Then, the total mean scores

for each treatment group were calculated. The evaluation criteria considered the solutions as non-irritant for values ranging within 0-3.9, slightly irritant for values ranging within 4.0-8.9, moderately irritant for values ranging within 9.0-12.9, and seriously irritant for values ranging within 13-16 [1].

2.9.2 Establishment of the FK rabbit model

Fifteen healthy, 8-week-old New Zealand white rabbits (weighting 1.5-2.0 kg) were selected from the Animal Center of the First Affiliated Hospital of Harbin Medical University. Each animal had a corneal thickness of greater than 500 μm. These animals were fed for one week before model preparation for adaptation. The animal room reached the specific pathogen free (SPF) standard. All procedures were approved by the Ethics Committee of Harbin Medical University and conducted according to the guidelines of the ARVO statement for the Use of Animals in Ophthalmic and Vision Research.

The rabbits were kept under observation for 72 hours to exclude any local or systemic diseases. General anesthesia was induced in these rabbits by intravenous injection of 1 ml/kg of 3% sodium pentobarbital. Topical anesthesia was achieved with two drops of oxybuprocaine hydrochloride (Benoxil). A 30-gauge insulin needle was used to create a corneal incision at approximately 0.1 mm in depth in the right eye of each rabbit. A 100-μL aliquot of the inoculums, which contained 400×10^4 CFU/ml of *C. albicans* was circularly injected into the superficial stroma of rabbit eyes [29],[30]. Antibiotics (tobramycin and dexamethasone eye ointment, and levofloxacin eye drops) were administered to the eyes after surgery for three times a day for 15 days, in order to prevent bacterial growth.

At 48 hours after inoculation, these animals were divided into three treatment groups, with five rabbit eyes in each group: control (Ctrl) group, treated with saline solution for eight times a day (8 am to 4 pm, one drop per hour) up to 15 days; Low frequency of Nat group, treated with topical natamycin for three times a day (8 am to 4 pm, one drop every four hours) up to 15 days; Nat group, treated with topical natamycin for eight times a day (8 am to 4 pm, one drop per hour) up to 15 days; natamycin-loaded micelle (Nat-Mi) group, treated with natamycin-loaded micelle for three times a day (8 am to 4 pm, one drop every four hours) up to 15 days. The concentration of natamycin in the Nat-Mi group was adjusted to be consistent with that of the Nat group by calculation.

The eyes of each group was clinically examined and recorded using a slit lamp on day 5, 10 and 15. Confocal microscopy and optical coherence tomography (OCT) were used for the examination and photographically recorded the examination on day 5 and 15. At the end of the 15 days, animals were euthanized by intravenous injection of sodium pentobarbital (150 mg/mL) in the marginal ear vein. Then, the eyes were enucleated and immediately frozen on dry ice: isopentane bath. Afterwards, hematoxylin and eosin (H&E) staining and fungal culture (on day 15) were conducted after the corneas were dissected in frozen condition.

2.9.3 Slit lamp observation

The SLM-8E digital slit lamp analysis system (KANGHUA, Chongqing, China) was used to observe the conjunctival hyperemia, corneal clouding, corneal infiltration (measured as the size of the epithelial defect in mm), corneal neovascularization and hypopyon level. The rabbits were anesthetized using sodium pentobarbital and

oxybuprocaine hydrochloride. Then, the eyes were evaluated at baseline and random time points after injection by slit-lamp biomicroscopy.

The clinical scoring was performed after slit lamp examination. Parameters, such as conjunctival hyperemia, corneal clouding, corneal infiltration (measured as the size of the epithelial defect in mm), corneal neovascularization and hypopyon level, were evaluated and noted in each rabbit. The clinical score was determined with a brief modification through the following Schreiber scoring system. In brief, the conjunctival hyperemia was graded, as follows: 0, no; 1, mild; 2, medium; 3, high grade hyperemia. The corneal clouding was graded, as follows: 0, no clouding or clear cornea; 1, mild clouding; 2, corneal clouding in two quadrants of the cornea; 3, total corneal clouding. Corneal neovascularization was graded as 0, no; 1, mild (≤2 mm from the limbus); 2, medium (>2 mm from the limbus); 3, high (until the center of the cornea) neovascularization. The corneal infiltrate and hypopyon diameter were measured using the largest diameter in millimeters [31].

2.9.4 Direct smear

The corneal specimens were scrapped from the corneal surface using an ophthalmic scraper, placed on the clean slide, and stained with H&E dye. Then, the slide was gently warmed and directly examined under a microscope to check for the presence of fungus.

2.9.5 Confocal microscopy observation

Confocal laser microscopy (Heidelberg Engineering GmbH, Heidelberg, Germany) was used to directly observe fungus. Each rabbit eyelid was opened using an eye speculum, and an assistant fixed the rabbit head in position. All camera

settings were maintained constant throughout the experiment. For each examination, the repeated through-focus data sets were obtained from the corneal region to identify the presence of fungus.

2.9.6 Anterior segment optical coherence tomography examination

The anterior segment optical coherence tomography (AS-OCT) system (Optovue, CA, USA) was used to assess the corneal thickness. The rabbits were anesthetized, and the pupils were dilated with 1% tropicamide solution. The corneas were frequently lubricated during the imaging session. Afterwards, these rabbits were placed in a restrainer for stability, and a pediatric probe was used for optical coherence tomography (OCT) analysis. Then, 6-mm horizontal line scans in the inferior retina below the optic disk were used to capture the corneal cross-sections.

2.9.7 H&E staining

Histological examination was used to observe the fungal hyphae, integrity and regularity of the cornea, inflammatory cells, and neovascularization. The left half of each cornea was fixed in buffered formalin, embedded in paraffin wax, cut at 5-μm sections, and stained with H&E dye.

2.9.8 Fungal culture of corneas

The *C. albicans* colony scrapped from several corneas were observed by *in-vitro* culture. Briefly, the left (right) half of each cornea was homogenized in sterile PBS using a homogenizer. Then, the supernatant was collected by centrifugation, and diluted for 10 times. Afterwards, a series of dilutions of samples were spread on YPD plates for 48-hour incubation at 37℃.

2.10 LC-MS/MS analysis

Aqueous humor was collected using 30-gauge insulin needles, and the corneas were tailored by ophthalmic scissors on an ice bath. Then, these corneas were washed with PBS and homogenized using a hand homogenizer in cold methanol (1:10 w/v), with 10 μL of 10 μg/mL of amphotericin B (internal standard) added in the cornea homogenate. Afterwards, the homogenate was vortexed for one minute, placed in a sonic oscillator for 10 minutes, and subjected to centrifugation at 4,000 × g for 10 minutes to separate the supernatant. Then, the separated supernatant evaporated under nitrogen, and the residue after the evaporation was reconstituted in 100 μL of the mobile phase and subjected for LC-MS/MS analysis. Subsequently, 10 μL of 10 μg/mL of amphotericin B was added to 50 μL of aqueous humor, and 200 μL of acetonitrile was used to extract the analyte from the samples. The supernatant was subjected for analysis after 4,000 × g of centrifugation for five minutes. All steps were performed on ice, as much as possible.

The concentration of natamycin in the study samples was measured through the LC-MS/MS. The AB SCIEX QTRAP® 4500 triple-quadrupole mass-spectrometric system (AB Sciex, MA, USA) coupled with ultrafast liquid chromatography (AB Sciex, MA, USA) was used. The analytes were separated on the Bridge® BEH C18 column (4.6×150 mm, 2.5 μm) using 10 mM of ammonium formate in water and acetonitrile as the mobile phase at a ratio of 60:40 (v/v), and pumped at 0.6 mL/min. The multiple reaction monitoring (MRM) of natamycin was analyzed using an electrospray in positive ion mode. The MRM transition was 666.3 → 503.4 and 924.5 → 906.6 (IS). The source was operated at 400°C with an electrospray voltage of 5,500 V. The ion source parameters were as follows: curtain gas 35 L/min, GS1 35,

GS2 50, and CAD gas 6 L/min. The standard curve ranged from 10 ng/mL to 5,000 ng/mL.

2.11 Statistical analysis

The values were presented as mean ± standard deviation (SD). The differences were analyzed using one-way analysis of variance (ANOVA), followed by *t*-test for the pairwise comparison of subgroups. These statistical analyses were performed using the SPSS software (v13.0; SPSS, Inc., Chicago, IL, USA), and a *P*-value of <0.05 was considered statistically significant.

3. Results and Discussion

3.1 Synthesis and characterization of the PEG-*b*-PGMA copolymer

A general strategy for the synthesise of PEG-*b*-PGMA is illustrated in **Figure 1**. The macro-TTC was first synthesized via the EDC/DMAP coupling reaction. The preparation of PEG-based chain transfer agent (macro-TTC) was verified by analyzing the corresponding peaks in the ^{1}H NMR spectra (**Figure S1**). The number-average molecular weight (M_n^{GPC}) of 6.9 kDa with a dispersity ($Đ$) of 1.07 was determined for macro-TTC by GPC (**Figure S2**). Then, the block copolymer PEG-*b*-PGMA was synthesized *via* the RAFT polymerization of glycidyl methacrylate (GMA) using the prepared macro-TTC. After 19 hours of polymerization, near quantitative conversion of GMA (*ca.* 99%, 30 GMA units) was achieved through ^{1}H NMR analysis (**Figure S1**). The GPC curve revealed a monomodal peak (M_n^{GPC} of 11.9 kDa) and a narrow dispersity ($Đ$ = 1.23), suggesting a controlled polymerization (**Figure S2**).

3.2 Self-assembly and characterization of micelle

The PEG-*b*-PGMA copolymer comprised of hydrophilic and hydrophobic segments. The PEG segments provide solubility within aqueous environments, and PGMA segments offer drug loading capacity for hydrophobic drugs. The self-assembly of PEG-*b*-PGMA was achieved through the solvation of the block copolymer in THF, followed by the dropwise addition of EtOH as a non-solvent for the PGMA segment (**Figure 2**). The subsequent removal of THF was achieved by dialysis (MWCO = 3.5 k) against EtOH. The resultant nanoparticles (*NP*) assembled in EtOH displayed a hydrodynamic diameter (D_H) of approximately 200 nm by DLS measurement (**Figure S3**). The self-assembled structures tended to rapidly disassemble at concentrations below the critical association concentration and/or under external stimuli (e.g. temperature, pH and light) [32]. For drug delivery applications, it is often necessary to stabilize the structures to prevent the undesired burst release of the encapsulated cargo/drug. Therefore, in order to stabilize the micelle in the present study, 1,7-diaminoheptane was used as a cross-linker to covalently stabilize the assembled structures through the nucleophilic attack of 50 mol% of the total epoxy rings available (**Figure 2**). After stabilization, the cross-linked nanoparticle (*XL-NP*) was dialyzed (MWCO = 3,500 g/mol) against EtOH to remove any unreacted cross-linker. Then, DLS measurements were conducted to present the micelle size after cross-linking. As shown in **Figure 3A**, the non-cross-linked micelle dissolved in THF (no Tyndall effect, insert-i) and recovered the block polymers with a D_H of 2.5 nm, which agrees well with the measuring size of the PEG-*b*-PGMA coil in THF. In contrast, cross-linked micelle (*XL-NP*) exhibited an enlarged D_H of 294 nm in THF, when compared to the value obtained in EtOH (D_H of 190 nm

with Tyndall effect, insert-ii), suggesting that the covalent cross-linking of micelle was successful.

In order to visualize the morphology of the cross-linked micelle, TEM was utilized (**Figure 3B**). From the TEM image, distinct spherical solid structures with average diameters (D^{TEM}) of approximately 160 nm could be observed, which is in good agreement with the size (190 nm) obtained from the DLS measurements (**Figure 3A**). Based on the literature, polymeric micelle is commonly known as *ca.* 20-70 nm in diameter. However, the sizes obtained in the present work were considerably larger (*ca*. 160-190 nm). It is likely that these particles represent "crew-cut" multi-core micelle, in which the dimensions of the hydrophobic core are much larger than the corona [33].

3.3 Investigation of the hydrolysis of the glycidyl groups

Due to the presence of the remaining glycidyl groups (50 mol%, 15 repeat units) in the hydrophobic core, the micelles are designed to undergo hydrolysis with the presence of H_2O as a nucleophile. **Figure 4** presents the ^{1}H NMR spectroscopic analysis of the *in situ* hydrolysis of glycidyl units under mild physiological conditions (PBS pH 7.4, 37°C) for over eight days. After eight days of incubation, the proton resonance peak ***c***, which corresponds to the glycidyl units of PGMA, underwent a change in resolution (**Figure 4A** *vs.* **4B**), suggesting that partial hydrolysis, as peaks ***b*** and ***c***, were still present in the spectrum (consistent with the reports in the literature) [34]. Upon integration of the newly formed resonance ***c'*** of the hydrolyzed PEG-*b*-PGMA (methylene group, 2H, -CHC***H***$_2$OH-; **Figure 4B**) *vs.* resonance ***c*** of the PEG-*b*-PGMA (methylene group, 2H, -OC***H***$_2$CH$_2$-; **Figure 4A**), it could be measured that ca. 53% of the total available PGMA groups has been hydrolyzed after eight days.

These results clearly show that the hydrolysis of the glycidyl groups occurs in physiological conditions, and causes the structural changes, in which two hydroxyl groups are produced from the nucleophilic attack of the epoxy ring. This would increase the inherent hydrophilicity of the hydrophobic core regions of the micelle, which could be utilized for drug delivery applications. The hydrolysis of the glycidyl groups has been widely used to gain extra functionality [35],[36], but to the best of our knowledge the application of this simple process has not been explored as an endogenous stimulus for sustained drug release. In addition, the hydrolysis of the glycidyl groups is commonly achieved under harsh conditions (i.e. 80°C in H_2SO_4), which does not mimic the physiological conditions [37]. However, this study revealed that the hydrolysis of the glycidyl groups could occur under mild physiological conditions (PBS pH 7.4, 37°C) over a longer period of time, which makes it suitable for the sustained release of hydrophobic drugs at physiological conditions.

3.4 *In vitro* drug loading and drug release

Natamycin, which is a hydrophobic antifungal drug, was encapsulated inside the cross-linked micelle (*nat-NP*, **Figure 2**). Briefly, natamycin was dissolved in DMSO (a good solvent for both drug and micelle), added dropwise into the cross-linked micelle suspension in ethanol, and left mixing. This helps the drug to be trapped inside the hydrophobic core of the cross-linked micelle. Then, the solution was dialyzed against PBS to further induce drug entrapment and remove any organic solvent. UV-Vis spectroscopy was used to calculate the amount of free drug in the solution using standard curves generated from known drug concentrations. The DLE and DLC were 94.1% and 15.8%, respectively. The high drug loadings of micelle can be attributed to the large size of the cross-linked micelle and the multicore structure

(**Figure 5A**). Drug-loaded micelle exhibited a size of $Đ^{TEM}$ of approximately 160 nm in the TEM image (**Figure 5A)**, which is in close agreement with the size of micelle observed in the DLS and TEM before drug loading (**Figure 3**). The *in vitro* release of natamycin from the micelle was subsequently investigated under physiological conditions (PBS pH 7.4, 37°C), which mimics the ocular environment. A rapid initial release (approximately 18%) was observed within 20 hours, followed by a plateau (**Figure 5B**). After eight days, a maximum of *ca*. 34% drug released from the micelle. The burst release within the first 20 hours can be attributed to the release of attached or loosely trapped free drugs. The release of the other 16% of natamycin over eight days could be attributed to the hydrolysis of the hydrophobic glycidyl groups, resulting hydroxyl groups. This could increase the hydrophilicity of the micelle core and thus "pushes" the encapsulated hydrophobic cargo out of the assemblies. Natamycin release in this study could occur due to two driving forces: (i) the concentration driven release (ii), and the change in inherent hydrophilicity of the assemblies.

3.4 Cytotoxicity of natamycin-loaded micelle *in-vitro*

In order to study the biocompatibility of drug-loaded micelle (*nat-NP*), the cytotoxicity was investigated by CCK-8 assay. The toxicity of natamycin-loaded micelle (Nat-Mi group) were compared with that of the pure natamycin in PBS (Nat group). The concentration of natamycin in the Nat-Mi group was consistently adjusted with that in the Nat group. From the *in vitro* drug release curve, a *ca*. 18% rapid release can be observed within 20 hours, followed by a plateau with a total *ca*. 34% cumulative release in eight days (**Figure 5B**). However, 8-day cell culture was too long due to the contact inhibition, while 72 hours (*ca*. 31% release) was more

suitable. Hence, 24 hours (rapid release phase) for the short-term toxicity test and 72 hours (slow release phase) for the long-term toxicity test were chosen. As shown in **Figure 6**, after 24 and 72 hours of exposure, the cell viability in the Nat-Mi group and Nat group was not statistically different, when compared to the control group (P>0.05). In addition, at the same concentration of natamycin, the viability of these two groups was not different (P>0.05). These results imply that all substances including natamycin, micelle, and natamycin-loaded micelle were nontoxic to epithelium at all tested concentrations. Thus, the drug-loaded micelle is a biocompatible carrier for ocular drug transportation.

3.5 Anti-fungal effect of natamycin-loaded micelle *in-vitro*

Since the loaded drug in the micelle was an anti-fungal drug, its anti-fungal ability was detected to determine whether the released drug was still effective. Prior to quantitative experiments, several qualitative studies were carried out to measure the minimal inhibition concentration (MIC) and inhibition zone diameters of *Candida albicans,* which is the safest fungus for laboratory culture isolated from FK eyes.

The MIC represented the lowest drug concentration that inhibited fungus growth after 18-24 hours of incubation. The lower the MIC values, the stronger the anti-fungal ability. In the present study, the MIC values in the Nat-Mi group were compared with those in the Nat group and control group. The positive control contained the media and fungus, while the negative control contained only the media. In addition, it needs to be emphasized that the drug-loaded micelle was stored at 37°C to achieve maximal release prior to the MIC experiment. After 24 hours of incubation, the absorbance of each group at 600 nm were determined. As shown in **Figure 7**, the

concentration where the number of fungus reduces to zero and inhibits the fungus growth is represented as the MIC values. The MIC values of micelle (25 mg mL^{-1}, containing 4 mg mL^{-1} of natamycin) were similar to that of pure natamycin (2 mg mL^{-1}), suggesting that the ability of drug-loaded micelle was slightly weaker when compared to pure natamycin, although drug was fully released from the micelle prior to the performing experiment.

In addition, the inhibition diameter of 9.65 ± 0.65 mm and 14.19 ± 1.08 mm were observed for pure natamycin at dilutions of 25 μg and 50 μg, respectively. Slightly smaller zone of inhibitions 9.09 ± 0.66 mm and 13.85 ± 0.95 mm were found for drug-loaded micelle after 24 hours of incubation (**Figure 7B**). From the obtained results of the MIC values and the diameter of inhibition zone, a similar but slightly lower anti-fungal activity of natamycin-loaded micelle was observed when compared to pure natamycin. Micelle, as a drug carrier, have no anti-fungal ability to *Candida albicans.* Hence, it can be concluded that all fungal inhibitions resulted from the natamycin released from micelle. The slightly lower antifungal activity may be attributed to the restriction by the micelle structure and the incomplete release of drug from the micelle.

3.6 Cytotoxicity of natamycin-loaded micelle *in-vivo*

We have performed *in vitro* experiments to show that drug-loaded micelle is non-toxic. Here, the ocular irritation was evaluated using the modified Draize test to investigate the cytotoxicity of the natamycin-loaded micelle *in vivo*. Natamycin-loaded micelle were instilled into the left eyes, while blank PBS were instilled into the right eyes, which was used as controls. After three days of instillation, no significant eye reaction (such as corneal opacity, iris hyperemi, conjunctival congestion, swelling

and discharge) was observed in the Nat-Mi group (80 mg mL^{-1}). The total clinical score was 0, indicating that natamycin-loaded micelle does not cause irritation, and are non-toxic *in vivo* (**Figure S4**).

3.7 Anti-fungal effects of natamycin-loaded micelle *in-vivo* -- clinical observation

In order to determine the therapeutic effect of natamycin-loaded micelle, general clinical evaluation was performed under a slit lamp. FK animal models were established through the injection of a *C. albicans* colony into the corneal stroma.

The representative images of infected cornea with *Candida albicans* which was treated with natamycin-loaded micelle (3 times/day), natamycin (normal frequency: 8 times/day, low frequency: 3 times/day) and untreated eyes over 15 days are presented in **Figure 8**. A slit lamp was used to observe the conjunctival hyperemia, corneal clouding, corneal infiltration, corneal neovascularization and hypopyon level of the eyes. On the day of inoculation, all experimental eyes instantly exhibited the development of conjunctival hyperemia. Pertaining to the corneal clouding, moderate clouding was observed in the low frequency of Nat group, Nat group and Nat-Mi group at day 5 after treatment (grade 2). In contrast, the rabbit eyes in the Ctrl group (grade 3) presented with severe clouding, and even invisible iris due to the diffuse of the corneal edema. At day 10, almost no clouding in the Nat group (grade 0) and mild clouding in the low frequency of Nat group (grade 1) and Nat-Mi group (only in the bottom right corner) (grade 1) was noted. At day 15, no clouding could be observed in the Nat group (grade 0) and Nat-Mi group (grade 0), and a small part remained in the low frequency of Nat group (grade 1). However, more and more serious clouding appeared in the Ctrl group as the cornea became non-transparent at day 15 (grade 3).

For the corneal infiltration, rabbit eyes in the Nat group and Nat-Mi group presented with 2.118 ± 0.353 mm and 1.829 ± 0.198 mm corneal lesions at day 5, respectively. At day 10, 80% of the corneal lesions in the two groups regressed to ≤1 mm. And it was completely and clinically recovered by the end of the treatment (day 15). For the Ctrl group, the highest level of corneal lesion diameter (2.250 ± 0.375 mm, 2.723 ± 0.365 mm, and 5.143 ± 1.029 mm at day 5, 10, and 15, respectively) was observed during all the examination time. Corneal lesions in the low frequency of Nat group shrunken gradually but left 1.937 ± 0.379 mm and were not completely healed at day 15.

At day 5, the Nat-Mi group had the narrowest corneal neovascularization ring followed by the Nat group < low frequency of Nat group < Ctrl group, but all groups were less than 2 mm from the limbus (grade 1). At day 10, a remarkable increase of neovascularization was observed in the Ctrl group (grade 2, >2 mm from the limbus), while regression was displayed in the low frequency of Nat group (grade 1), Nat group (grade 0), and Nat-Mi group (grade 0). Furthermore, the neovascularization in the Ctrl group progressed to the center of the cornea and even covered the entire eyes (grade 3, day 15). At low frequency of Nat group, a circle of new blood vessels still remained (grade 1).

For the height of the hypopyon-fluid level in the Nat group and Nat-Mi group, it was no more than one-fifth of the rabbit eye diameter at day 5 (2.483 ± 0.717 mm and 2.519 ± 0.513 mm, respectively). And the hypopyon in this two groups were disappeared from the beginning of day 10. Similarly, hypopyon in low frequency of Nat was also decreased but a small part remained at day 15 (0.280 ± 0.159 mm). Nevertheless, the hypopyon-fluid level in the Ctrl group increased from day 5 (3.143

± 0.655 mm) to day 10 (5.333 ± 0.611 mm), and after 15 days this became full of pus in the anterior chamber (10.519 ± 0.679 mm) (**Figure 8A**).

Clinical score was calculated as the calculation of the total scores as the sum of the five clinical parameters could better describe the process of clinical healing throughout the treatment period. As shown in **Figure 8B**, no statistical difference of the clinical scores were observed between the four groups at day 5 ($P>0.05$). At day 10, an increase of the mean clinical scores in the Ctrl group was observed ($P<0.05$). In contrast, a significant decrease of scores were observed in the low frequency of Nat group, Nat group and Nat-Mi group ($P<0.05$) while scores in the low frequency of Nat group was significantly higher than the other two groups ($P<0.05$). At the study endpoint (at day 15), the difference in clinical scores was more evident ($P<0.05$), and the scores in the Nat group and Nat-Mi group were close to zero. These results revealed that the use of natamycin-loaded micelle could reduce the frequent use of pure natamycin to 3 times per day, suggesting the improved sustained release of natamycin.

3.8 Anti-fungal effects of natamycin-loaded micelle *in-vivo* -- fungal numbers

Macro scale clinical observation in the previous section showed that FK could be treated by the application of natamycin-loaded micelle (3 times per day).; however, the micro scale changes need to be determined. Hence, in order to observe the microscopic changes of fungus, the methods of direct smear, confocal microscopic observation, and fungal culture were used. The use of direct smear method was the only qualitative experiment which provides a way to directly observe the appearance of the fungus. Corneal specimens were scrapped from the corneal surface and examined under a microscope after staining with the H&E dye. As shown in **Figure 9**,

the shape of the mature spores is similar to beads in all groups at day 5, indicating infection of all groups by *Candida albicans* infection. At day 15, spores were observed in the Ctrl group and low frequency of Nat group, while no fungus was found in the Nat group and Nat-Mi group, indicating that the infection was controlled in the last two groups.

In order to quantitatively measure the numbers and distribution of fungus, confocal microscopy was used. Intravital confocal microscopy is the gold standard for the diagnosis of bacterial or fungal infection in clinic. Fungal structures in rabbit corneas were recorded at day 5 and 15 (**Figure 9**). The examination revealed highly reflective, linear, branching and bifurcating fungal structures in all groups at day 5.A significant amount of fungus was presented in the Ctrl group while less numbers were found in the low frequency of Nat group, followed by Nat group and Nat-Mi group (**Figure 9**). Due to the persistent antifungal treatment, fungal structures in the Nat group and Nat-Mi group were progressively reduced, and finally disappeared in the corneas at day 15. Fungus in the low frequency of Nat group were also decreased but were not eliminated completely at day 15.

Fungal cells grow very fast and exponentially. A small amount of fungus can be ignored easily under microscopy, but can be noticed easily by amplification test *in-vitro*. Therefore, fungal culture was used to further confirm whether there were invisible fungal residues in the Nat group and Nat-Mi group under microscopes or not. The supernatant from the homogenized cornea were cultured on YPD plates. After 48 hours of culture, plates remained clean in the Nat group and Nat-Mi group. However, a number of white spherical fungus cells were observed in the Ctrl group and low frequency of Nat group (**Figure S5**).

The obtained results from the above three methods suggest that the improvement of keratitis attributes to the reduction in fungal cell numbers and proves that the anti-fungal effect of natamycin-loaded micelle (3 times/day) was equal to pure natamycin (8 times/day).

3.9 The anti-fungal effect of natamycin-loaded micelle *in-vivo* -- corneal morphology

Since the fungal numbers were decreased after the natamycin-loaded micelle treatment, the corneal morphology was expected to be improved from the micro perspective as well. The corneal morphology was recorded through anterior segment optical coherence tomography (AS-OCT) and H&E staining. OCT is a new technology for detecting light scattering signals from different layers of eye tissues through the principle of a weakly coherent light interferometer. Keratitis could cause corneal stromal edema and leads to the increase in central corneal thickness and inflammatory infiltration which could be recorded by AS-OCT. In addition, epithelial layer, basal layer, and stromal layer could also be observed through the AS-OCT examination. As shown in **Figure 10**, at day 5, deficient epitheliums, shallow basal layer, diffused high reflection signal in stroma, increased central corneal thickness (443.67 ± 13.20 μm, 465.82 ± 24.26 μm, 470.33 ± 20.13 μm, and 485.33 ± 21.08 μm, respectively), and *ca.* 50% corneal infiltration were observed in all groups. In particular, a small amount of gray-white substance which was assumed to be purulent secretion in the anterior chamber was observed in the Ctrl group, implying serious damage of the corneas. After another 10 days of treatment (day 15), the corneal thickness in the Ctrl group was increased to 736.67 ± 14.36 μm, while in the low frequency of Nat group, Nat group and Nat-Mi group were decreased to 406.84 ±

743 18.96 μm, 317.00 ± 14.11 μm, and 351.00 ± 9.54 μm, respectively. Depth of corneal
744 infiltration was significantly decreased with no fungal lesions were observed in the
745 Nat group and Nat-Mi group; however, a lesion was still existed with half depth of
746 corneas in the low frequency of Nat group at day 15. Nevertheless, the depth of lesion
747 was enhanced to the full-thickness of the corneas in the Ctrl group with a large
748 number of purulent secretions in the anterior chamber at day 15.
749 On the histopathological examination, mixed inflammatory reactions including
750 the presence of polymorphonuclear cells, lymphocytes and plasma cells, both inside
751 and around the infiltrate were recorded in the control specimens at day 15. In addition,
752 a numerous superficial and deep vascular reaction with endothelium on the vascular
753 wall and erythrocytes inside vascular wall were also observed in the Ctrl group. The
754 presence of *Candida* pseudofilaments in the corneal epithelium and stroma directly
755 implied severe fungal infections in rabbit eyes. Less inflammatory cells, angiogenesis,
756 and pseudofilaments in the low frequency of Nat group could be found at day 15.
757 Very low inflammatory reactions and absence of angiogenesis and fungi were
758 observed in the Nat group and Nat-Mi group (**Figure 10**). These results show that the
759 natamycin treatment could improve the corneal morphology of keratitis through the
760 sustained drug release from the micelle which was similar to the use of pure
761 natamycin.
762
763 **3.10 Natamycin-loaded micelle promote drug penetration *in vivo***
764 The present results revealed the use of less frequency of natamycin in the Nat-Mi
765 group could cure fungal keratitis with 15 days with a similar therapeutic effect with
766 the Nat group. Literatures have reported that micelle nanoparticles could enhance
767 drug penetration in the skin and tumor [38], [39]. Hence, it was expected that the

present PEG-*b*-PGMA micelle could increase natamycin penetration into the corneas and possess same concentration of drug in the lesions. In order to verify this assumption, LC-MS/MS was employed to measure the concentration of natamycin in the corneas and aqueous humor (a kind of liquid behind the cornea) of several groups. Natamycin could be recognized by MRM transition from 666.3 to 503.4 which means that the encapsulated natamycin in the micelle could not be detected by LC-MS/MS. Therefore, only free natamycin can been detected by LC-MS/MS. In **Figure 11**, it could be observed that after 15 days of treatment, the concentration of natamycin in the Nat-Mi group was similar to that in the Nat group in both the cornea and aqueous humor ($P>0.05$). In the low frequency of Nat group, the concentration of natamycin was much lower than the two groups ($P<0.05$). These results exhibit that the detected free amount of natamycin in the cornea and aqueous humor determine the effectiveness of the FK treatment. Additionally, it shows that the use of PEG-*b*-PGMA micelle could help the natamycin to penetrate into the cornea and deeper aqueous humor. The reason could be the improved mucoadhesion of micelles which can enhance the contact time with the mucus layer of the tear film and increase the corneal penetration due to the PEGylated shell of micelles as it has been also shown by previous researchers [23], [24], [40].

4. Conclusion

A drug carrier with sustained released characteristic for the ocular delivery system was developed to reduce the frequent doses of natamycin for FK treatment. Micelles were prepared *via* the self-assembly of PEG-*b*-PGMA block copolymer consisting of a hydrophilic PEG segments and a hydrolysable PGMA segments. Our results demonstrated that this new platform is capable of enhancing drug bioavailability and drug activity. The natamycin-loaded micelle system can

significantly enhance the loading and prolong delivery efficiency of drug in aqueous humor and cornea, and finally reduce the administration frequency to improve long-term patient compliance.

Acknowledge

This work was supported by The National Natural Science Foundation of China (81970776; 81671844) and The Scientific Research Transformation of Foundation of Heilongjiang Academy of Medical Sciences (CR201809). All authors acknowledge the funding provided by the Australian Research Council under the ARC Linkage Grant (LP150100315) and Heilongjiang Harbin Medical Pharmaceutical co. LTD.

Conflicts of interest

There are no conflicts of interest.

Reference

Figure legends

Figure 1 Schematic illustration of the synthesis of the PEG-*b*-PGMA copolymer.

Figure 2 Schematic illustration of (i) the preparation of self-assembled micelle using EtOH as the non-solvent, (ii) the cross-linking of nanoparticles *NP*, (iii) the hydrophobic drug loading of nanoparticles (*nat-NP*), and (iv) the self-hydrolysis induced drug release.

Figure 3 (A) DLS intensity average (D_H) measurements of non-cross-linked micelle in THF (green) and cross-linked micelle in EtOH (red) and THF (blue). The inset (ii) clearly represents the Tyndall effect of the cross-linked nanoparticles in THF; (B) TEM images of the cross-linked nanoparticles (*XL-NP*, multi-core micelle) (XL-NP was drop-casted from EtOH).

Figure 4 The ^{1}H NMR spectra of PEG-*b*-PGMA (A) before hydrolysis and (B) after eight days of hydrolysis in PBS at 37°C.

Figure 5 (A) TEM images of drug-loaded (or natamycin-loaded, Nat-NP) multicore micelle (Nat-NP was drop casted from PBS); (B) *In vitro* cumulative drug release percentage of natamycin with pH 7.4 at 37°C.

Figure 6 The natamycin-loaded micelle were non-toxic to corneal epithelial cells. The cell viability in the Nat group and Nat-Mi group was detected by CCK-8 after 24 hours (A) and 72 hours (B) of incubation. The data were expressed as mean ± standard deviation (SD), *n*=3. Ctrl = control, Nat = natamycin, Nat-Mi = natamycin-loaded micelle.

Figure 7 Natamycin-loaded micelle inhibited *Candida* growth *in vitro*. Minimal inhibition concentration (A) and the diameter of zone of inhibition (B) in the Nat-Mi group and Nat group against *Candida* were measured after 24 hours of incubation

838 in/on YPD medium. Ctrl1 = control 1, Ctrl2 = control 2, Nat = natamycin, Nat-Mi =
839 natamycin-loaded micelle.
840 **Figure 8** Natamycin-loaded micelle recovered the fungal keratitis in clinic. New
841 Zealand white rabbits were infected with *Candida albicans* and were routinely and
842 visually evaluated for corneal involvement for 15 days under a slit lamp. The control
843 group comprised of untreated fungal keratitis rabbits, while the remaining rabbits
844 were given anti-fungal drugs. A score was assigned for each of the following five
845 criteria: conjunctival hyperemia, corneal clouding, corneal infiltration (measured as
846 the size of epithelial defect in mm), corneal neovascularization and hypopyon level.
847 For the 15 consecutive days of observation, the representative images (A) and clinical
848 score measurements (B) are shown. The images indicate the disease progression at 5,
849 10 and 15 days. **P*<0.05, compared with the Ctrl group at the same time point;
850 #*P*<0.05, compared with same group at day five; n=3. Ctrl = control, Nat =
851 natamycin, Nat-Mi = natamycin-loaded micelle.
852 **Figure 9** Natamycin-loaded micelle reduced the fungal numbers *in vivo*. The fungal
853 morphology and numbers were observed with direct smear (left) and confocal
854 microscopy (right) at 5 and 15 days. Scale bars: 10 μm for left, 100 μm for right, *n*=3.
855 Ctrl = control, Nat = natamycin, Nat-Mi = natamycin-loaded micelle.
856 **Figure 10** Natamycin-loaded micelle improved the corneal morphology *in vivo*. The
857 corneal morphology was observed by anterior segment optical coherence tomography
858 (AS-OCT) (left) and H&E staining (right). Scale bars: 500 μm for left, 100 μm for
859 righ, *n*=3. Ctrl = control, Nat = natamycin, Nat-Mi = natamycin-loaded micelle.
860 **Figure 11** Natamycin-loaded micelle promoted the drug penetration *in vivo*. The drug
861 levels in eye tissues including the cornea (A) and aqueous humor (B) were detected at
862 the end of 15 days of post-dosing. **P*<0.05, compared with the Ctrl group; $^{\#}$*P*<0.05,

compared with the Nat group; *n*=3. Ctrl = control, Nat = natamycin, Nat-Mi = natamycin-loaded micelle.

Figures

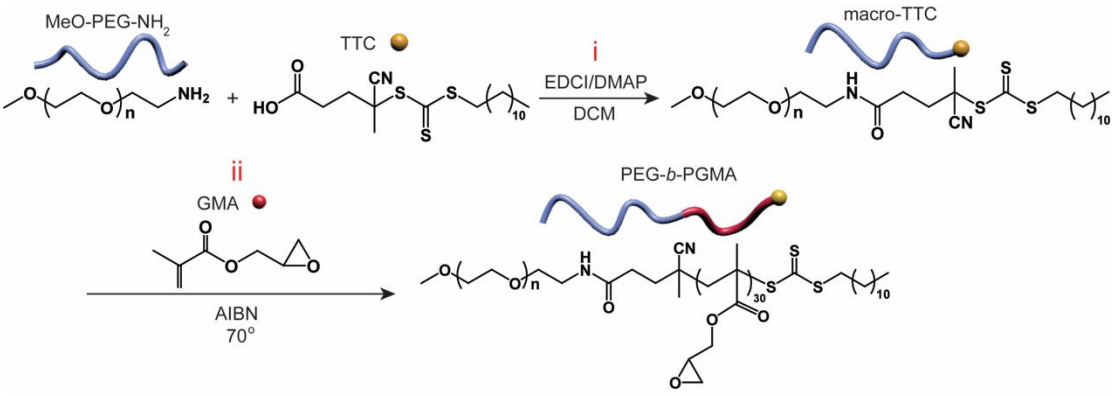

Figure 1

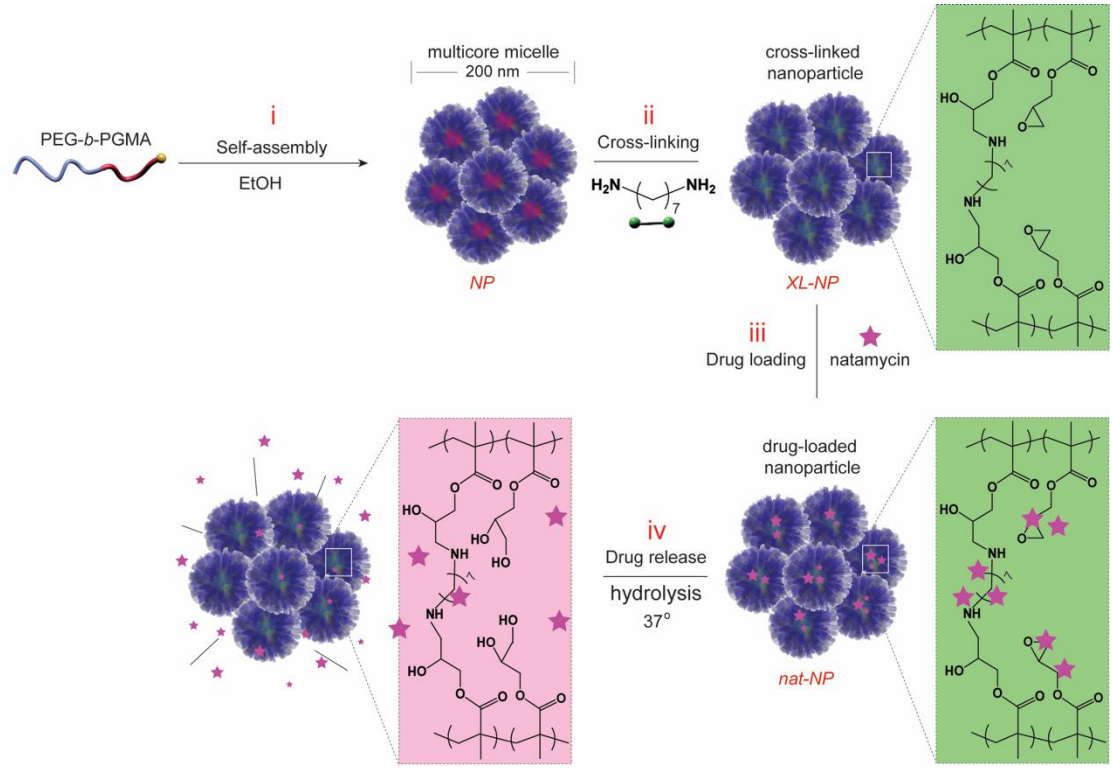

Figure 2

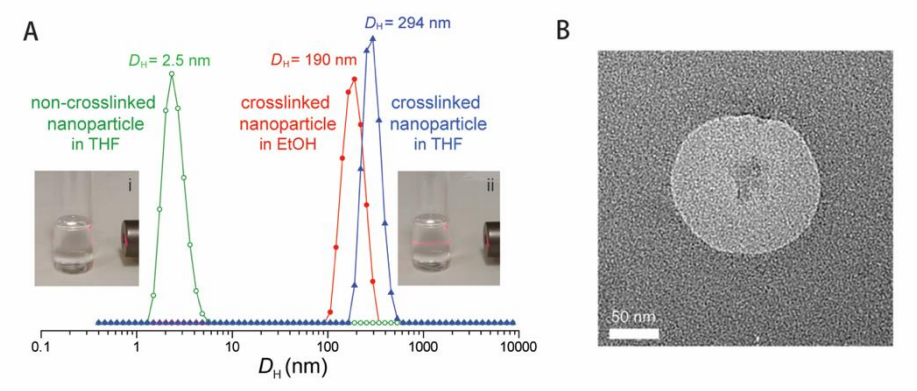

871

872 Figure 3

873

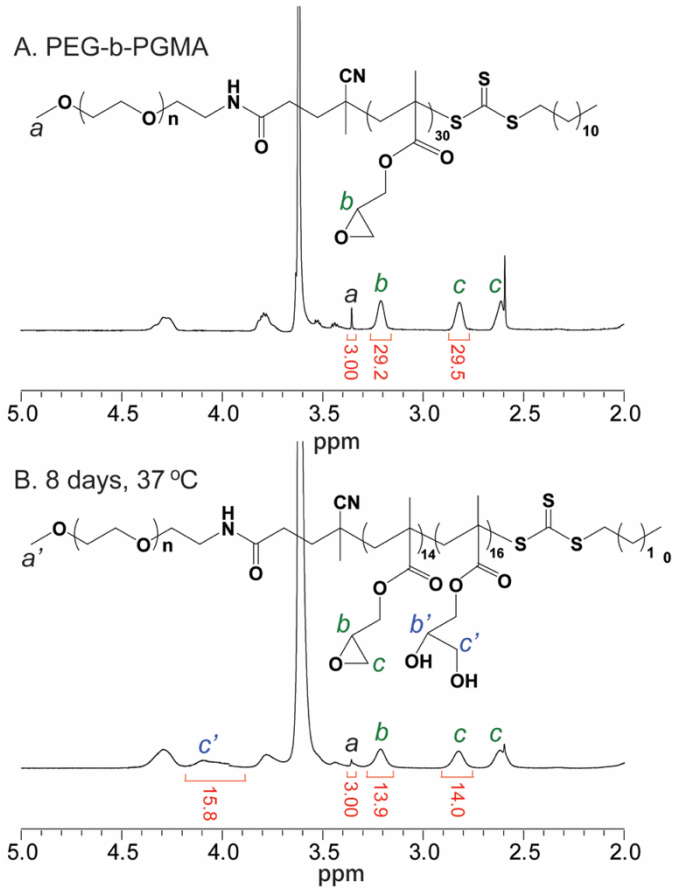

874

875 Figure 4

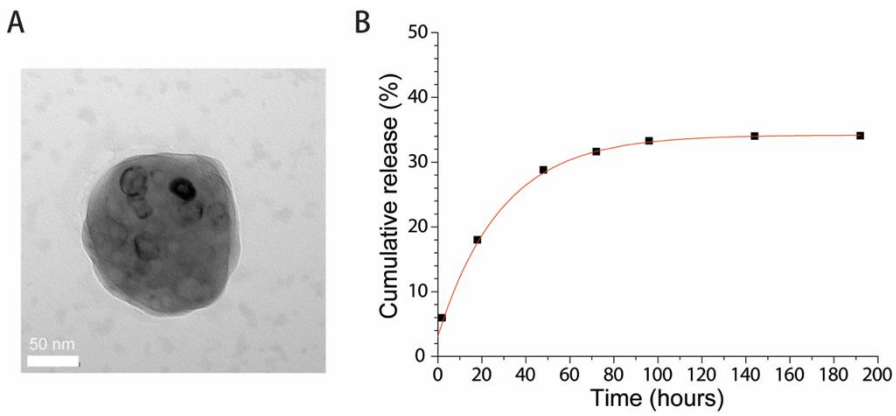
A
B
50 nm
Cumulative release (%)
Time (hours)
0
10
20
30
40
50
0
20
40
60
80
100
120
140
160
180
200

Figure 5

881

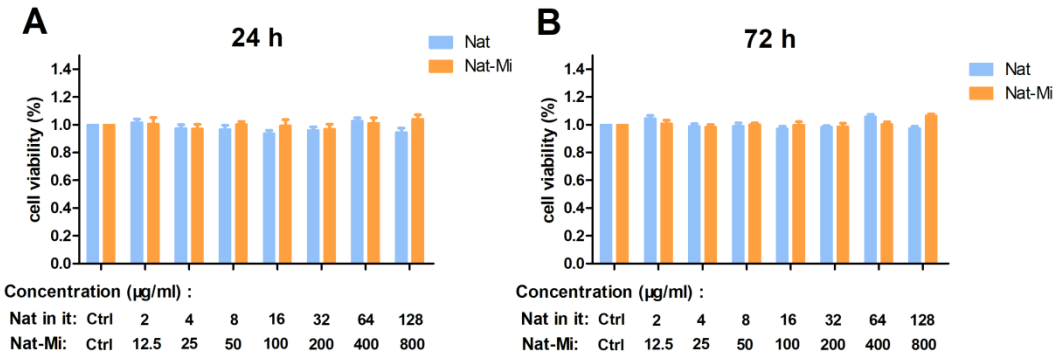

882

883 Figure 6

884

885

886

887

888 Figure 7

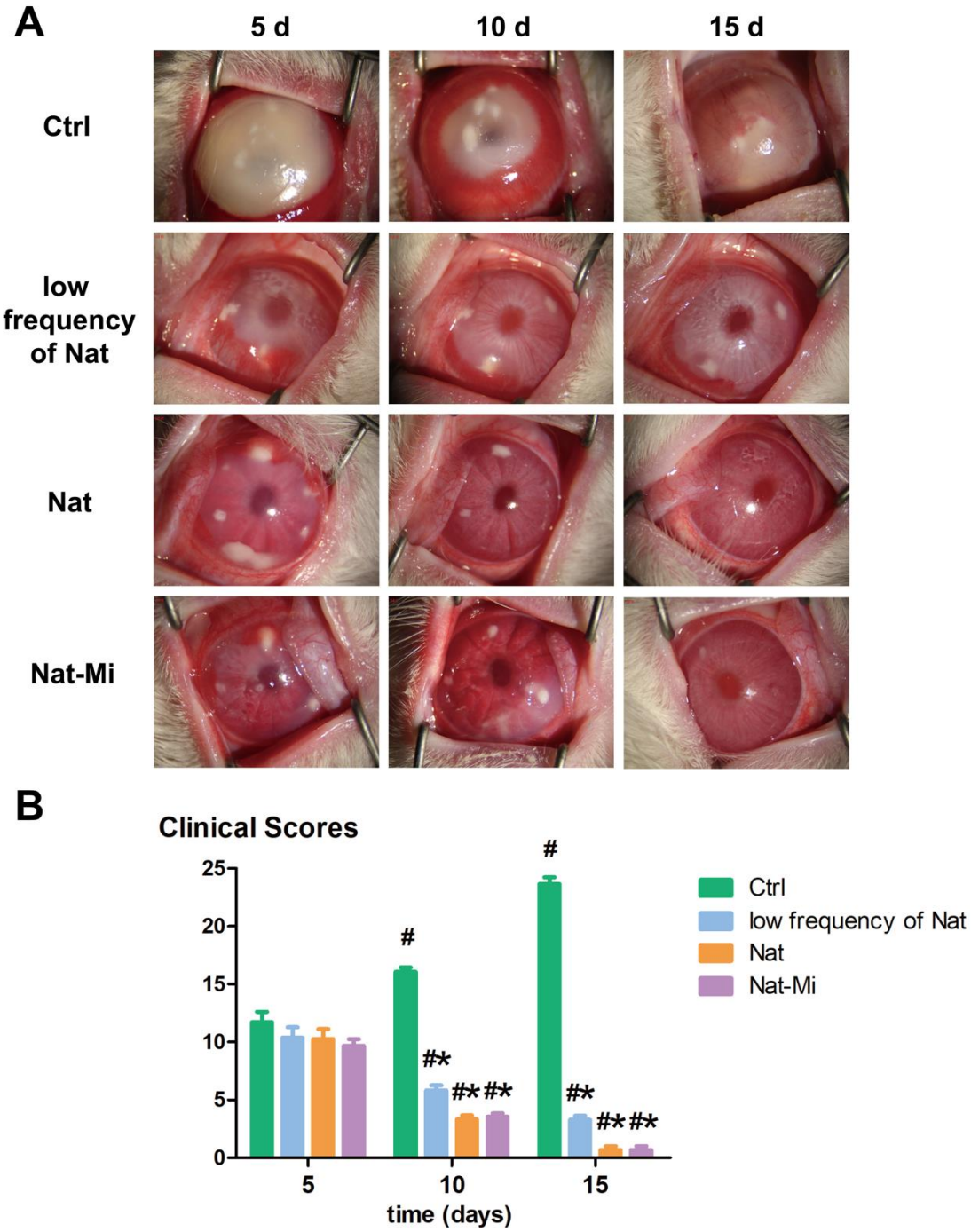
A
5 d
10 d
15 d
Ctrl
low frequency of Nat
Nat
Nat-Mi
B
Clinical Scores
25
20
15
10
5
0
5
10
15
time (days)
Ctrl
low frequency of Nat
Nat
Nat-Mi

Figure 8

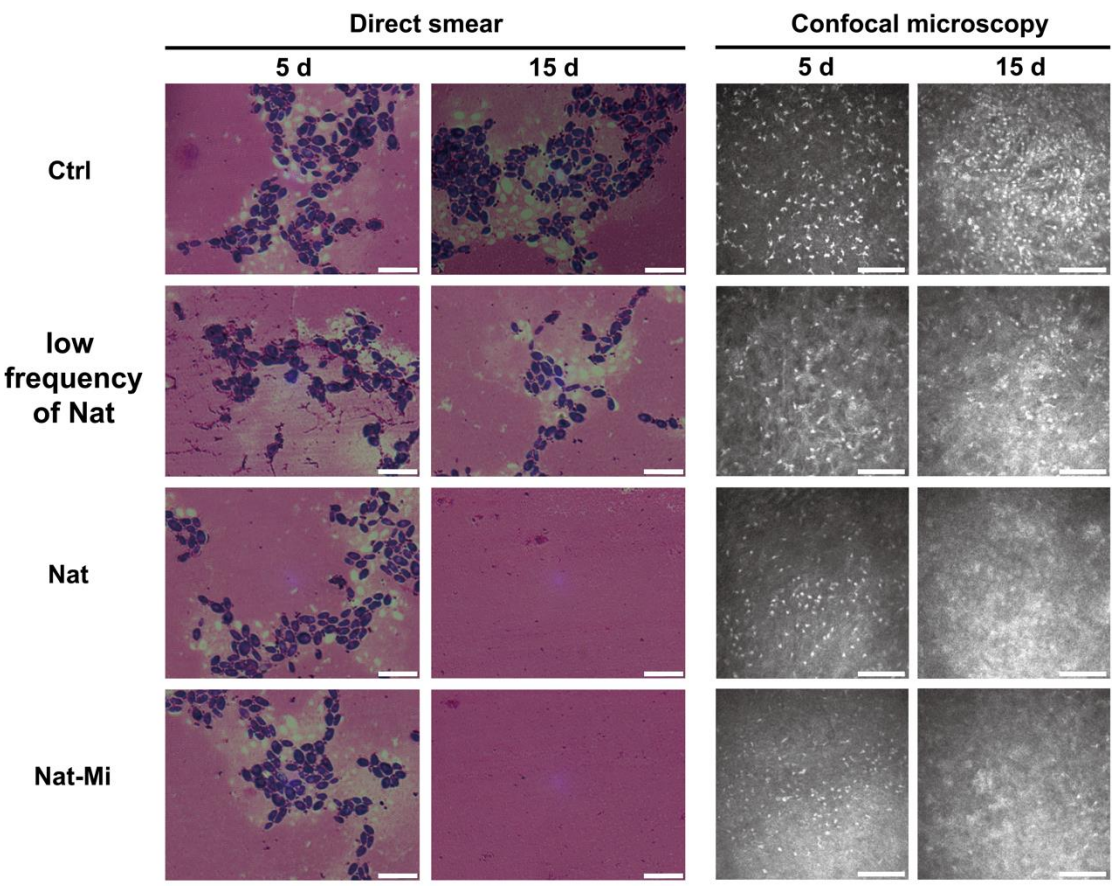

892

893 Figure 9

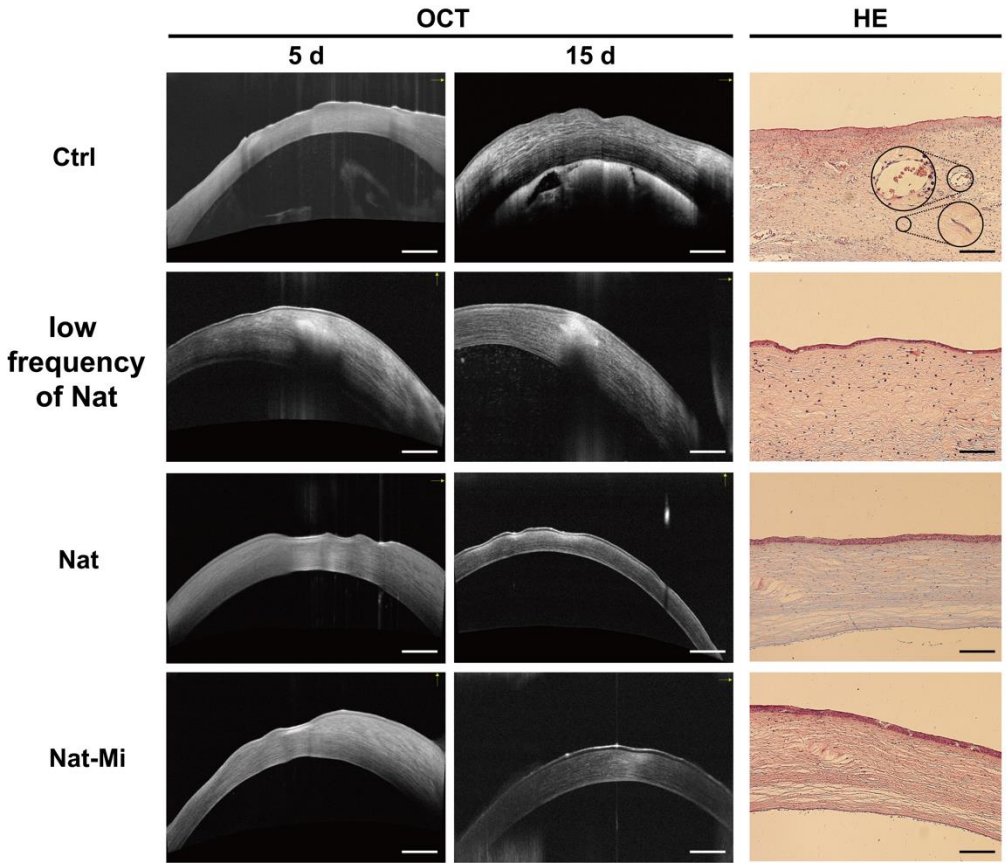

Figure 10

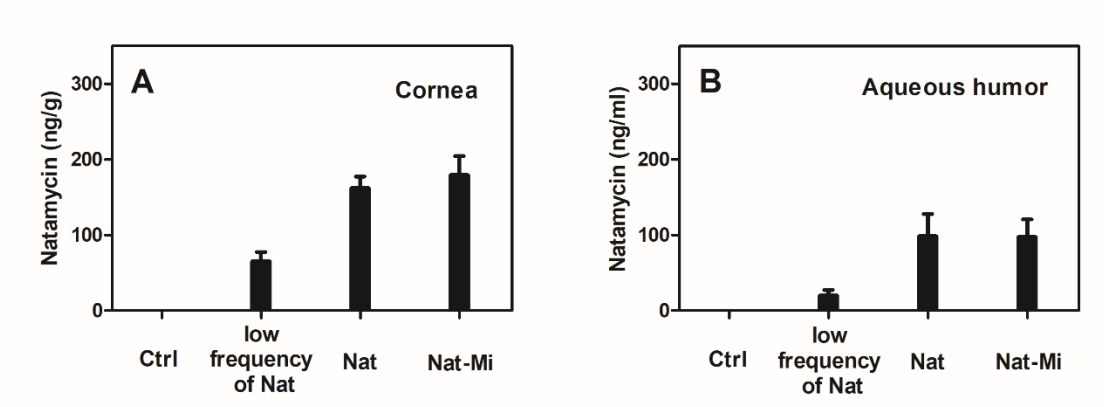

Figure 11

[1] H. Chandasana, Y.D. Prasad, Y.S. Chhonker, T.K. Chaitanya, N.N. Mishra, K. Mitra, P.K. Shukla, R.S. Bhatta, Corneal targeted nanoparticles for sustained natamycin delivery and their PK/PD indices: An approach to reduce dose and dosing frequency, Int J Pharm 477(1-2) (2014) 317-325.
[2] Y.S. Chhonker, Y.D. Prasad, H. Chandasana, A. Vishvkarma, K. Mitra, P.K. Shukla, R.S. Bhatta, Amphotericin-B entrapped lecithin/chitosan nanoparticles for prolonged ocular application, International Journal of Biological Macromolecules 72 (2015) 1451-1458.
[3] L. Niu, X. Liu, Z. Ma, Y. Yin, L. Sun, L. Yang, Y. Zheng, Fungal keratitis: Pathogenesis, diagnosis and prevention, Microb Pathog 138 (2019) 103802-103802.
[4] R.S. Bhatta, H. Chandasana, Y.S. Chhonker, C. Rathi, D. Kumar, K. Mitra, P.K. Shukla, Mucoadhesive nanoparticles for prolonged ocular delivery of natamycin: In vitro and pharmacokinetics studies, International Journal of Pharmaceutics 432(1-2) (2012) 105-112.
[5] O. Spierer, J. Dugar, D. Miller, T.P. O'Brien, Comparative antifungal susceptibility analysis of Candida albicans versus non-albicans Candida corneal isolates, Cornea 34(5) (2015) 576-579.
[6] P. Caffrey, J.F. Aparicio, F. Malpartida, S.B. Zotchev, Biosynthetic engineering of polyene macrolides towards generation of improved antifungal and antiparasitic agents, Curr Top Med Chem 8(8) (2008) 639-653.
[7] USFDA, 2008. NDA 50-514/S-009 Page 3 NATACYN1 (natamycin ophthalmic suspension)
https://www.accessdata.fda.gov/drugsatfda_docs/label/2008/050514s009lbl.pdf (accessed 31.05.14)
[8] B. Anjali, D. Prashant, R. Vinod, U. Kumud, Evaluation of cyclodextrins for enhancing corneal penetration of natamycin eye drops, Journal of Pharmacy & Bioallied Sciences 4(Suppl 1) (2012) S29-S30.
[9] C.-M. Phan, L.N. Subbaraman, L. Jones, In vitro\\r drug release of natamycin from β-cyclodextrin and 2-hydroxypropyl-β-cyclodextrin-functionalized contact lens materials, Journal of Biomaterials Science Polymer Edition 25(17) 1907-1919.
[10] A. Jain, S.G. Shah, A. Chugh, Cell Penetrating Peptides as Efficient Nanocarriers for Delivery of Antifungal Compound, Natamycin for the Treatment of Fungal Keratitis, Pharmaceutical Research 32(6) (2015) 1-11.
[11] C. Amit, S. Muralikumar, S. Janaki, M. Lakshmipathy, K.L. Therese, V. Umashankar, P. Padmanabhan, J. Narayanan, Designing and enhancing the antifungal activity of corneal specific cell penetrating peptide using gelatin hydrogel delivery system, Int J Nanomedicine (2019).
[12] P. Chau-Minh, L.N. Subbaraman, J. Lyndon, In vitro drug release of natamycin from β-cyclodextrin and 2-hydroxypropyl-β-cyclodextrin-functionalized contact lens materials, Journal of Biomaterials Science Polymer Edition 25(17) (2014) 1907-1919.
[13] I.O. de Solorzano, M. Prieto, G. Mendoza, V. Sebastian, M. Arruebo, Triggered drug release from hybrid thermoresponsive nanoparticles using near infrared light, Nanomedicine (Lond) (2019) 10.2217/nnm-2019-0270.

[14] K.M. Garland, S. Sevimli, K.V. Kilchrist, C.L. Duvall, R.S. Cook, J.T. Wilson, Microparticle Depots for Controlled and Sustained Release of Endosomolytic Nanoparticles, Cell Mol Bioeng 12(5) (2019) 429-442.
[15] Z. Wu, M. Duan, D. Xiong, C.Y. Zhang, Mesoscale Simulations of pH-Responsive Amphiphilic Polymeric Micelles for Oral Drug Delivery, Pharmaceutics 11(12) (2019) E620.
[16] G. Qu, S. Hou, D. Qu, C. Tian, J. Zhu, L. Xue, C. Ju, C. Zhang, Self-assembled micelles based on N-octyl-N'-phthalyl-O-phosphoryl chitosan derivative as an effective oral carrier of paclitaxel, Carbohydrate Polymers.
[17] T. Zhou, L. Zhu, H. Xia, J. He, S. Liu, S. He, L. Wang, J. Zhang, Micelle carriers based on macrogol 15 hydroxystearate for ocular delivery of terbinafine hydrochloride: In vitro characterization and in vivo permeation, European Journal of Pharmaceutical Sciences 109 (2017).
[18] Y. Mai, A. Eisenberg, Self-assembly of block copolymers, Chem Soc Rev 41(18) (2012) 5969-5985.
[19] Y. Lin, A. Böker, J. He, K. Sill, H. Xiang, C. Abetz, X. Li, J. Wang, T. Emrick, S. Long, Q. Wang, A. Balazs, T.P. Russell, Self-directed self-assembly of nanoparticle/copolymer mixtures, Nature 434(7029) (2005) 55-59.
[20] E.B. Figueroa-Ochoa, E.M. Villar-Alvarez, A. Cambón, D. Mistry, J. Llovo, D. Attwood, S. Barbosa, J.F.A. Soltero, P. Taboada, Lenghty reverse poly(butylene oxide)-poly(ethylene oxide)-poly(butylene oxide) polymeric micelles and gels for sustained release of antifungal drugs, International Journal of Pharmaceutics 510(1) (2016) 17-29.
[21] M.A. Gauthier, M.I. Gibson, H.-A. Klok, Synthesis of functional polymers by post-polymerization modification, Angew Chem Int Ed Engl 48(1) (2009) 48-58.
[22] M. Benaglia, A. Alberti, L. Giorgini, F. Magnoni, S. Tozzi, Poly(glycidyl methacrylate): a highly versatile polymeric building block for post-polymerization modifications, Polymer Chemistry 4 (2012).
[23] E.A. Mun, P.W.J. Morrison, A.C. Williams, V.V. Khutoryanskiy, On the Barrier Properties of the Cornea: A Microscopy Study of the Penetration of Fluorescently Labeled Nanoparticles, Polymers, and Sodium Fluorescein, Mol Pharm 11(10) 3556-3564.
[24] J. Li, L. Zhanrong, Z. Tianyang, Z. Junjie, X. Huiyun, L. Heng, H. Jijun, H. Siyu, W. Liya, Positively charged micelles based on a triblock copolymer demonstrate enhanced corneal penetration, Int J Nanomedicine 6027-.
[25] F. Karimi, T.G. Mckenzie, A.J. O'Connor, G.G. Qiao, D.E. Heath, Nano-scale clustering of integrin-binding ligands regulates endothelial cell adhesion, migration, and endothelialization rate: novel materials for small diameter vascular graft applications, Journal of Materials Chemistry B 5 (2017).
[26] F. Karimi, V.J. Thombare, C.A. Hutton, A.J. O'Connor, G.G. Qiao, D.E. Heath, Beyond RGD; nanoclusters of syndecan- and integrin-binding ligands synergistically enhance cell/material interactions, Biomaterials.
[27] W.R. Kirkpatrick, R.K. Mcatee, S.G. Revankar, A.W. Fothergill, D.I. Mccarthy, M.G. Rinaldi, T.F. Patterson, Comparative evaluation of National Committee for Clinical

Laboratory Standards broth macrodilution and agar dilution screening methods for testing fluconazole susceptibility of Cryptococcus neoformans, Journal of Clinical Microbiology 36(5) (1998) 1330-1332.
[28] G. Xiang-Chun, Q. Hui-Ping, B. Jian-Hai, H. Lei, C. Hao, Effects of oleic acid on the corneal permeability of compounds and evaluation of its ocular irritation of rabbit eyes, Current Eye Research 39(12) (2014) 1161-8.
[29] Y. Chen, W. Yang, M. Gao, M.W. Belin, H. Yu, J. Yu, Experimental study on cryotherapy for fungal corneal ulcer, Bmc Ophthalmology 15(1) (2015) 29.
[30] H.M. El-Mofty, M.A. Abdelhakim, M.F. El-Miligi, M.A. El-Nabarawi, I.A. Khalil, A New Combination Formula for Treatment of Fungal Keratitis: An Experimental Study, Journal of Ophthalmology,2014,(2014-4-29) 2014(4) (2014) 173298.
[31] K.C. Yoon, I.Y. Jeong, S.K. Im, H.J. Chae, S.Y. Yang, Therapeutic effect of intracameral amphotericin B injection in the treatment of fungal keratitis, Cornea 26(7) (2007) 814.
[32] M. Simona, N. Julien, C. Patrick, Stimuli-responsive nanocarriers for drug delivery, Nature Materials 12(11) (2013) 991-1003.
[33] L.F. Zhang, A. Eisenberg, Multiple Morphologies and Characteristics of Crew-Cut Micelle-Like Aggregates of Polystyrene-B-Poly(Acrylic Acid) Diblock Copolymers in Aqueous-Solutions, Journal of the American Chemical Society 118(13) (1996) 3168-3181.
[34] C.S. Gudipati, M.B.H. Tan, H. Hussain, L. Ye, C. He, T.P. Davis, Synthesis of Poly(glycidyl methacrylate)-block-Poly(pentafluorostyrene) by RAFT: Precursor to Novel Amphiphilic Poly(glyceryl methacrylate)-block-Poly(pentafluorostyrene), Macromolecular Rapid Communications 29(23) (2010) 1902-1907.
[35] M.A. Gauthier, M.I. Gibson, K. Harm-Anton, Synthesis of functional polymers by post-polymerization modification, Cheminform 40(13) (2010) 48-58.
[36] M. Benaglia, A. Alberti, L. Giorgini, F. Magnoni, S. Tozzi, Poly(glycidyl methacrylate): A highly versatile polymeric building block for post-polymerization modifications, Polymer Chemistry 4(1) (2013) 124-132.
[37] E.M. Muzammil, A. Khan, M.C. Stuparu, Post-polymerization modification reactions of poly(glycidyl methacrylate)s, RSC Advances 7(88) (2017) 55874-55884.
[38] B.S. Makhmalzade, F. Chavoshy, Polymeric micelles as cutaneous drug delivery system in normal skin and dermatological disorders, Journal of Advanced Pharmaceutical Technology & Research 9(1) (2018) 2-8.
[39] H. Liang, X. Ren, J. Qian, X. Zhang, L. Meng, X. Wang, L. Li, X. Fang, X. Sha, Size-Shifting Micelle Nanoclusters Based on a Cross-Linked and pH-Sensitive Framework for Enhanced Tumor Targeting and Deep Penetration Features, Acs Applied Materials & Interfaces 8(16) (2016) 10136-10146.
[40] F. Bongiovì, C. Fiorica, F.S. Palumbo, G. Di Prima, G. Giammona, G. Pitarresi, Imatinib-Loaded Micelles of Hyaluronic Acid Derivatives for Potential Treatment of Neovascular Ocular Diseases, Mol Pharm.